Proceedings of the ASME 2017 International Design Engineering Technical Conferences & Computers and Information in Engineering Conference
IDETC/CIE 2017
August 6-9, 2017, Cleveland, USA

DETC2017/MR-67364

REPORT OF ROBOTIC MACHINING MEASUREMENTS USING A STÄUBLI TX200 ROBOT: APPLICATION TO MILLING

Hoai Nam Huynh
Theoretical Mechanics, Dynamics and Vibration Unit
University of Mons, Mons, 7000, Belgium
Tel: 0032-65-374216, Fax: 0032-65-374183
Email: hoainam.huynh@umons.ac.be

Edouard Rivière-Lorphèvre
Olivier Verlinden*
Machine Design and Production Engineering Unit
University of Mons, Mons, 7000, Belgium
Tel: 0032-65-374547, Fax: 0032-65-374545
Email: edouard.riviere@umons.ac.be

ABSTRACT

One of the most promising manufacturing technologies nowadays is certainly the material removal using an industrial robot. Robotic machining is a fast growing technology as the number of robots used in industry is increasing continuously. Robots are indeed flexible which allows them to deal with large workpieces. On the other hand, their low stiffness restricts their use to machining operations accommodating a low accuracy or involving limited cutting forces as milling instabilities are more likely to occur. Since the impact of the machining process on the robot structure is not fully understood at this time, this paper aims to provide an in-depth analysis of experimental data obtained while machining an aluminium plate with a Stäubli robot arm. After describing the experimental set-up, three different analyses (metrological, vibration, cutting forces) were carried out on the basis of the machined workpiece and the measured signals. An identification of the cutting coefficients was eventually performed in order to fit a cutting force model to the measurements. Simulation results showed a good correlation with the experimental measurements.

NOMENCLATURE

a_e, a_p Radial and axial depth of cut [mm].
F_x, F_y, F_z Force components in X, Y and Z directions [N].
K_{tc}, K_{rc}, K_{ac} Cutting coefficients in tangential, radial and axial directions [MPa].

INTRODUCTION

The use of robotic systems generally transforms the way manufacturing processes are considered. In robotic machining, the typical CNC machine tool is replaced by an industrial robot upon which a spindle is mounted at its end-effector. This growing technology offers number of benefits compared to the use of conventional machine tool [1]. As a matter of fact, the versatility of industrial robots enables them to deal with large workspace at a very competitive cost. It is estimated that the cost saving lies around 30 % when comparing the prices of an industrial robot and a CNC machine tool having the same workspace [2]. In addition to their attractive cost, the agility of industrial robots allows them processing workpiece with complex shapes and difficult access. Machining robots may also help increasing the productivity of some operations (e.g.: manual operations such as chamfering, cleaning and trimming) and reducing the scrap rate. On the other hand, one of the major hurdles preventing the usage of machining robots in industry is their lack of stiffness at joints causing the structure to vibrate under the effect of cutting forces. It is indeed commonly accepted in the literature that the stiffness of an industrial robot lies around 1 [N/μm] while the same quantity for a CNC machine tool is much larger and is often beyond 50 [N/μm]; similarly, robot first natural frequencies reach values

*Same affiliation as first author: olivier.verlinden@umons.ac.be

between 10 and 20 [Hz] while for a CNC machine tool, they are generally between 100 and 1000 [Hz] [3]. Consequently, this low robot stiffness may even lead to the phenomenon called “chatter” in which a specific combination of the cutting parameters (e.g.: axial depth of cut and spindle speed) triggers a sharp increase in cutting forces and in vibrations. Hence, chatter is one of the major reasons preventing the adoption of robots for machining processes [4].

Concerning the fields of application nowadays, this technology is really profitable for process dealing with large workpieces like those found in aeronautics or in foundry [5]. Common machining operations include pre-machining, grinding, polishing, roughing, sanding, contouring, deburring and drilling in rather soft materials such as foam, wood, plastic and aluminium. In other words, all cutting operations tolerating a low accuracy or involving limited cutting forces although some researchers are trying to improve the quality of resulting parts in steel [6], composite [7], and in other hard materials.

On the research side, more and more papers are issued regarding the interaction of the manufacturing process and the industrial robot in order to commonly adopt someday robots for material removal processes. Current research covers topics such as the modelling and the identification of industrial robots for machining applications [8], the development of dynamic robot model to assess the milling operation stability [9], the identification of joint stiffness [10], the implementation of off-line compensation method for cutting force-induced errors [11], the improvement of machining performance through real-time deformation compensation [5].

This paper presents an analysis of results obtained through a campaign of measurements using a Stäubli TX200 machining robot. The milling operation to be considered was the surfacing of an aluminium plate under different axial depths of cut. After computing the trajectories of the robot using a *CAM* software, machining tests were carried out while measuring both the vibration level near the spindle and the cutting forces near the workpiece. The retrieved signals were then analysed in order to identify the cutting coefficients and the modal characteristics of the robot. The identified values were eventually adopted to fit a cutting force model to the measurements; the main goal of this paper being to feed the robotic machining community with new experimental data.

This paper is organized as follows: following this introduction section, the next section presents a review of the experimental set-up (the workpiece, the milling trajectories, the machining robot and the sensors). Then, three different analyses are carried out:

- a metrological analysis;
- a vibration analysis;
- a cutting force analysis.

They are followed by the fitting of a cutting force model to the measurements using, inter alia, a finite element model of the robot to roughly assess its modal characteristics. The paper ends with a summary of the machining tests along with a discussion for future work.

EXPERIMENTAL SET-UP

This first section introduces the established experimental set-up in order to achieve the milling tests. It is divided in three subsections and successively covers a description of the milling operations, the machining robot and the acquisition systems.

Milling operations

The considered workpiece was a plate in aluminium alloy 6082 T6 whose dimensions are 100x90x10 [mm]. Four through holes were drilled so that the plate could be secured on the cutting force sensor later on (Fig. 1).

FIGURE 1: Aluminium 6082 T6 plate: 100x90x10 [mm]

The surfacing operations are illustrated in figure 2. As can be seen, just a portion of the whole surface was machined. The area where the material was removed corresponded to a rectangle of 50x90 [mm].

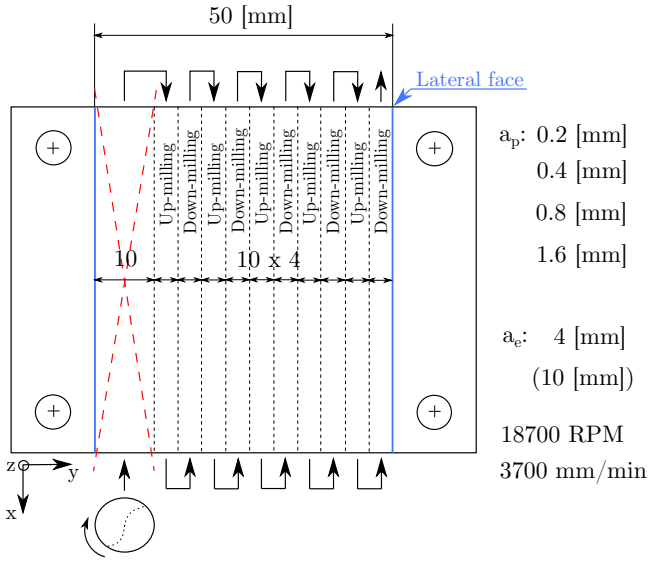

FIGURE 2: Milling trajectories and cutting conditions

The cutting tool followed a zigzag trajectory starting from one of the longitudinal edges: the first pass in the material was a slotting operation of 10 [mm] width followed by a succession of ten passes (alternatively in up-milling and in down-milling) with a radial depth of cut a_e=4 [mm]. Each layer of material was removed at a constant axial depth of cut. Five layers were cut out but, since the absolute positioning of the robot with respect to the part was questionable, it was decided to bound the study to the last four axial depths of cut. Also the slotting operation of each layer was dismissed of the study to only focus on ten passes with the same radial depth of cut. Table 1 summarizes the milling operations.

TABLE 1: SUMMARY OF THE MILLING OPERATIONS

Pass	a_p	a_e	Spindle speed	Feed speed
1	0.2	4.0	18700 [RPM]	3700 [mm/min]
2	0.4	4.0	18700 [RPM]	3700 [mm/min]
3	0.8	4.0	18700 [RPM]	3700 [mm/min]
4	1.6	4.0	18700 [RPM]	3700 [mm/min]

The milling trajectories were first computed in a *CAM* environment before being sent to the controller of the robot. In this framework, SprutCAM was used to generate the zigzag trajectory and its corresponding G-code. Attention can already be drawn on the fact that the robot modal characteristics will be studied for the particular configuration presented in figure 3.

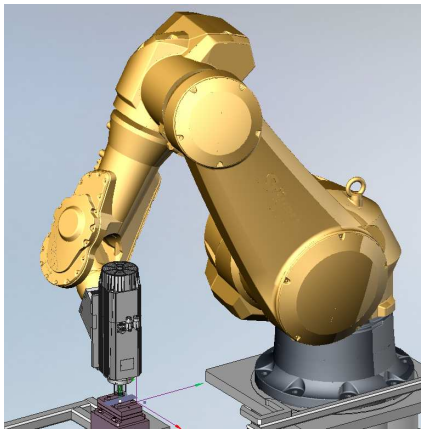

FIGURE 3: Computation of the trajectories in SprutCAM

Machining robot

In the present work, a robotic machining cell was set up with a Stäubli TX200 robot. This 6-DOF robot offers a nominal payload of 100 [kg] and a repeatability of $\pm$ 0.06 [mm]. The approximate height of the robot in the considered configuration was about 2 [m]. According to the manufacturer, its structure was enhanced to improve its stiffness, inter alia, thanks to in-house manufactured gearboxes. A TEKNOMOTOR milling spindle, whose maximum rotational speed reaches 24000 RPM, was mounted on robot wrist while the workpiece was fixed on a Kistler 9257B force sensor (Fig. 4).

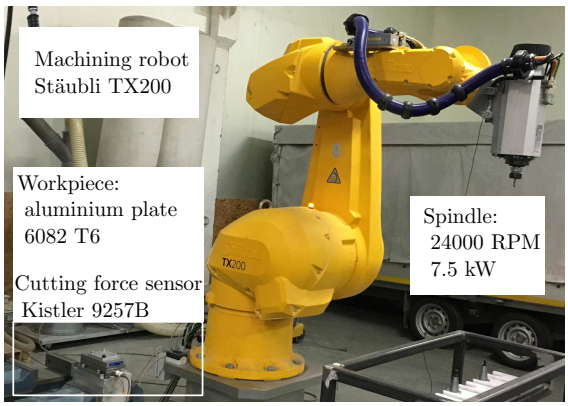

FIGURE 4: Experimental set-up

The characteristics of the milling tool are displayed in table 2. It is a 2-tooth carbide cutting tool from SECO TOOLS.

TABLE 2: MILLING TOOL CHARACTERISTICS

Diameter	Length	Helix angle	Nb tooth	Variable pitch
10 [mm]	75 [mm]	30°	2	170°-190°

Acquisition systems

Three different acquisition systems were used in order to monitor both the evolution of the cutting forces and the vibrations:

1. a tri-axis accelerometer was magnetised onto the surface of the interface part between the spindle and the robot wrist. It is a DYTRAN accelerometer whose frequency bandwidth

ranges up to 5000 [Hz] (Fig. 5). Only the signal along the feed direction was analysed in this study;

FIGURE 5: Spindle and tri-axis accelerometer

2. a second accelerometer (mono-axis) was glued on an aluminium block intended to fix the cutting force sensor on the top of its surface (Fig. 6). The support block was then fastened between the jaws of a vise. Its retrieved signal was unused in this study;
3. finally, a sensor measuring the cutting forces in x, y and z directions was mounted on top of the support surface. Its bandwidth reaches about 2000 [Hz] in x and y directions and is able to measure forces up to 5000 [N]. The workpiece was finally bolted to the sensor using four screws as shown in figure 6.

All the retrieved signals were sampled at 10000 [Hz].

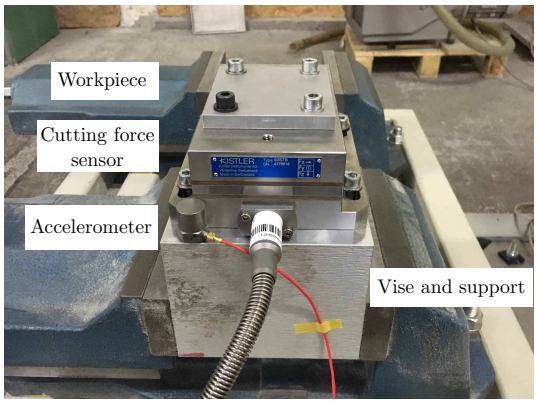

FIGURE 6: Measuring devices

METROLOGICAL ANALYSIS

The first analysis aimed to characterized the quality of the machined surface after the removal of all material layers (Fig. 7). Overall, the surface quality was better than it was expected from a machining robot; for instance, Schneider U. et al. showed, in an article issued in 2013, a photograph of a machined aluminium surface where the impact of gears backlash was clearly visible [12]. In this case, the machined surface was rather smooth to touch.

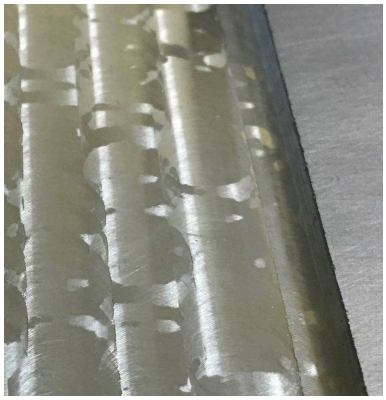

FIGURE 7: Machined surface

Five roughness measurements were achieved using a DIAVITE DH-6 portable roughness analyser along the grooves left by the tool in the feed direction. All measurements were accomplished using a cutoff wavelength of 0.8 [mm] (according to ISO 4288). The five grooves were analysed over a length of 4.8 [mm]. As seen in figure 8 for one of the analysed roughness profiles, the marks left by the feed of the milling tool are distinctly visible. The distance between two consecutive marks is approximately 0.25 [mm] while the expected feed per revolution was expected around 0.20 [mm] for a feed speed of 3700 [mm/min] at 18700 [RPM].

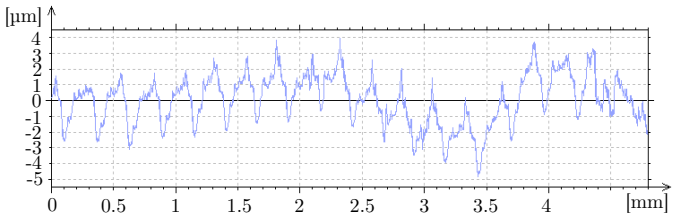

FIGURE 8: Roughness assessment along one machined groove

The mean values of arithmetic roughness and total roughness of the five profiles are displayed in table 3. This analysis was then completed by one roughness measurement for each lateral face. Building on results obtained, it can be inferred that the arithmetic roughness class lies between 0.4 and 0.8 μm. In fact, it is a quite impressive result since this range of roughness could be qualified as "fairly accurate" if it had been achieved by a machine tool. This level of accuracy is often dedicated for guidance and centring systems and mobile contacts.

TABLE 3: ROUGHNESS INDICATORS

	Arithmetic roughness R_a	Total roughness R_t
Bottom plane	0.693 (range 0.4-0.8) μm	6.0 μm
Lateral faces	0.596 (range 0.4-0.8) μm	12.7 μm

Finally, the flatness of the bottom surface was measured using a CMM machine WENZEL LH 54 according to ISO 11001-2004. The z coordinate of more than 4000 measurement points equally spaced was evaluated on the machined surface. A plane was then fitted to the point cloud and the flatness was assessed by the best RMS plane: a value of flatness of 0.238 [mm] was found. In figure 9, it can be observed that the roughness along the feed direction (along y in the figure) is better than the transverse one. It might be somehow linked to the variable configuration of the robot.

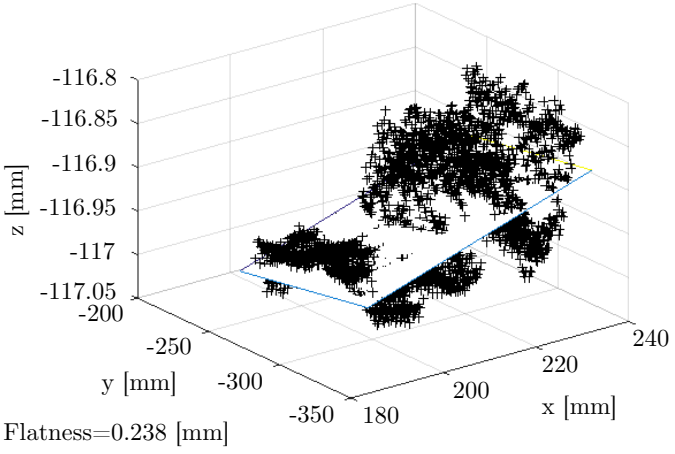

FIGURE 9: Flatness evaluated by best RMS plane

FREQUENCY ANALYSIS

A Fast Fourier Transform was applied to the vibration signals collected while milling. Figure 10 focusses on the FFT of a vibration signal along the feed direction for a down-milling pass at 1.6 mm depth since the analysis of the other signals yielded similar results.

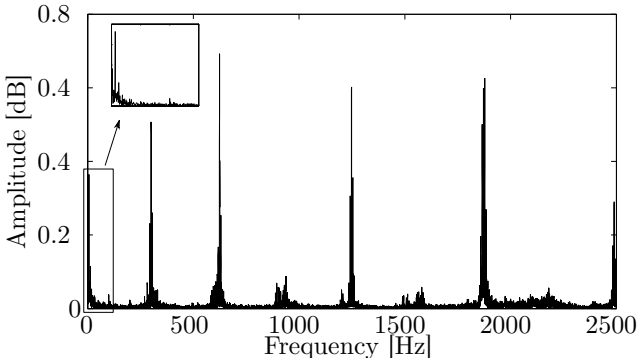

FIGURE 10: Fast Fourier Transform at a_p=1.6 [mm]

At first sight, the position of the frequency peaks, equally spaced every 312 [Hz], seems consistent with the programmed spindle speed of 18700 [RPM] bearing in mind that the cutting tool has two teeth and that harmonics also occur every 624 [Hz].

A closer look at the lower frequencies allows getting a glimpse of high peaks that might correspond to the resonances of the robot. Apparently, a frequency peak at 7 [Hz] seems to emerge and could refer to the first eigen frequency of the Stäubli robot. It wouldn't be incoherent since it is reported in the literature that the first robot frequencies are around 10 [Hz].

CUTTING FORCE ANALYSIS

Cutting force signals along x and y directions were analysed for the purpose of identifying the specific pressures defining any tool/workpiece material couples. In this study, a linear model of the cutting forces is assumed (Eq. 1) [13]:

$$\begin{aligned} dF_t &= K_{tc} \cdot h \cdot db \\ dF_r &= K_{rc} \cdot h \cdot db \\ dF_a &= K_{ac} \cdot h \cdot db \end{aligned} \tag{1}$$

with

- dF_t, dF_r, dF_a: infinitesimal tangential, radial and axial forces applied on each tooth;
- K_{tc}, K_{rc}, K_{ac}: cutting coefficients;
- h: undeformed chip thickness;
- db: projected length of an infinitesimal cutting flute in the direction along the cutting velocity.

This simple analytical model doesn't require any intensive calculation but the cutting coefficients K have no clear correlation with the intrinsic properties (e.g. Young's modulus and hardness/yield strength) of the considered material. As a result, machining experiments must be performed to determine them.

Rivière-Lorphèvre et al. [14] developed an inverse method for cutting coefficient evaluation for cutting tools of any type [15]. The latter performs a least square fitting on the basis of the measured cutting forces to retrieve the optimal cutting coefficients. During each fitting iteration, the cutting forces from the model are computed by a time and a spatial discretisation. The cutting tool is sliced into superimposed discs of elementary height. Thus, at each time step, the geometries of the tool and the workpiece are considered to compute the chip thickness leading to the cutting forces [16]. The fitting eventually provided the best cutting coefficients using a least square method.

The inverse method was applied to the steady state cutting force signals of each pass into the material. A total of 40 inverse fittings were carried out since there were 10 passes per axial depth of cut. Figure 11 depicts the fitting of the cutting force model to the measurements for a down-milling pass at a_p=1.6 [mm]. In order to obtain this clean fitting, the measured signals were first filtered through a low-pass filter with a cutoff frequency of 1000 [Hz]; half of the sensor bandwidth. Although the figure only presents the fitting over one tool revolution, the cutting forces measured over all tool turns are overlayed to figure out whether the model accords well.

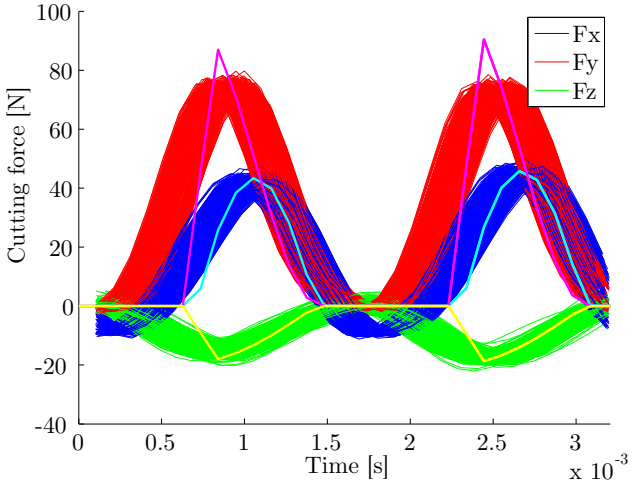

FIGURE 11: Machining model fitting at a_p=1.6 [mm] in down-milling

After examining all passes into the material, the identified cutting coefficients of each inverse analysis were plotted onto the same graph. Coefficient K_{ac} was omitted of the study as its identification is generally less accurate. In figure 12, the first 10 tests correspond to the successive up- and down-milling passes at a_p=0.2 [mm], and etc. As the axial depth of cut increases, the signal-to-noise ratio of the cutting force signals rises as well. Therefore, the values of the identified cutting coefficients tend to settle down. It appeared that the mean value for K_{tc} was 661.513 [MPa] while K_{rc} hardly stabilised around 253.458 [MPa], which were plausible values for aluminium.

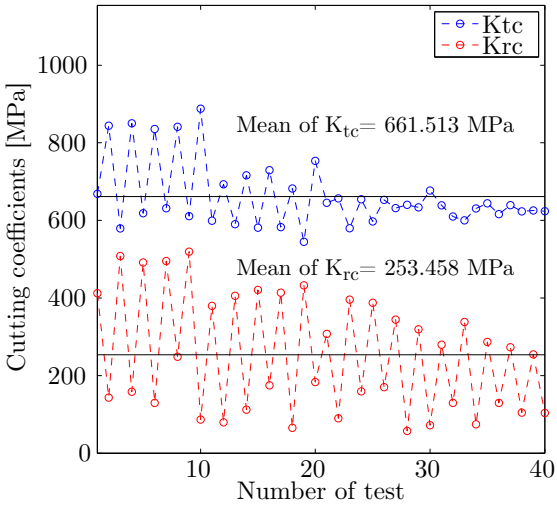

FIGURE 12: Cutting coefficient identification for aluminium

Figure 13 shows the evolution of cutting force F_x and F_y levels as the axial depth of cut increases for all down-milling operations.

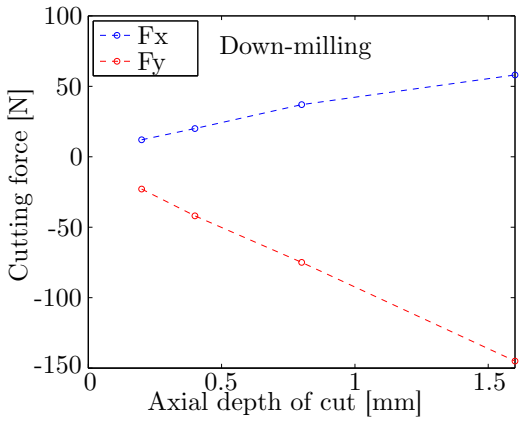

FIGURE 13: Down-milling: evolution of the cutting forces

The equivalent graph for the up-milling operations is drawn in figure 14.

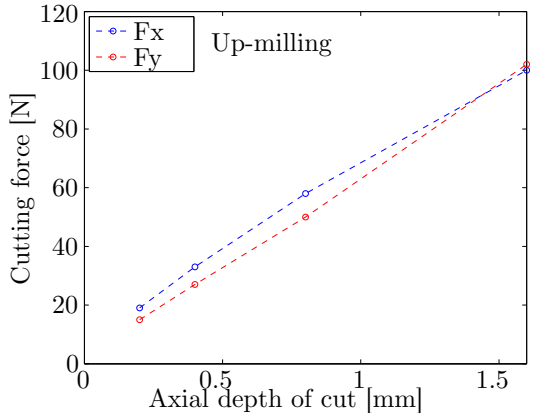

FIGURE 14: Up-milling: evolution of the cutting forces

The trends shown in figure 13 and 14 are usually expected since cutting forces rise linearly with the axial depth of cut.

MACHINING MODEL FITTING

The mean cutting coefficients obtained from the inverse analyses of all tests were eventually deployed to fit a cutting force model to the measurements. The considered model simplifies the machining process, the robot arm holding a spindle, to a mass-spring-damper system moving at a constant speed v into the material while reacting to the cutting forces (Fig. 15) [17]. Since the model allows incorporating dynamic effects, the damping ratio ξ and the modal mass m of the system were identified.

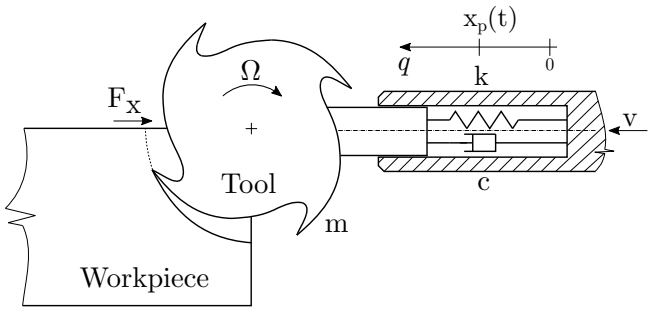

FIGURE 15: Single-DOF milling model

with

- Ω: spindle speed;
- m, c, k: mass, damping and stiffness of the whole robot;
- q: unique degree of freedom;
- x_p: equilibrium position of the spring;
- v: feed speed of the robot end-effector.

Damping identification

As with the cutting coefficients, the cutting force signals were again exploited to identify a global damping ratio ξ. To do so, the decline of each filtered cutting force signal along x- and y-directions was matched with an exponential decay as depicted in figure 16 for a down-milling pass at a_p=1.6 [mm].

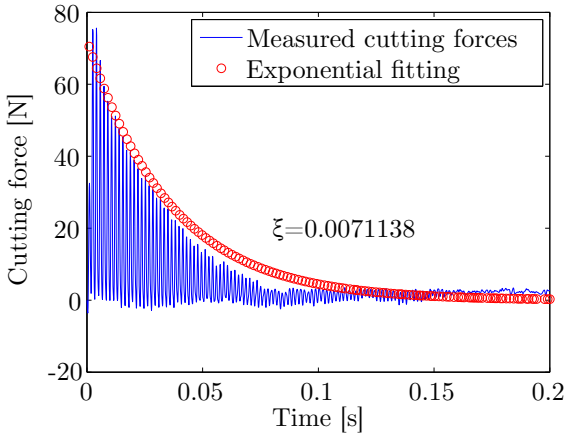

FIGURE 16: Damping identification at a_p=1.6 [mm]

The damping ratio is simply the exponent of the exponential and in that case, its value was ξ=0.0071. Having examined the cutting force decays of all depths of cut, it turned out that the mean damping ratios for x- and y-directions were both around ξ=0.005.

Modal mass identification

Since the experimental set-up was no longer available to perform a modal analysis, a finite element model was carried out on Abaqus software to identify a global modal mass corresponding to the first mode. The 3D model of the robot holding the spindle and the cutting tool was built using the provided 3D parts of manufacturers. Since 3D parts were sometimes difficult to mesh, they were simplified in order to remove any convoluted geometry and hollowed as it is the case for real robot arms. Standard tetrahedron elements (C3D10) of various sizes depending on the considered part were chosen: e.g. 15-mm-side elements were picked up to mesh the main arm while smaller elements were used to mesh the cutting tool. In this way, the computation time wasn't affected too badly. Structure assembly was made by imposing TIE constraints freezing all DOF between each parts. Different materials were assigned to the parts: tungsten carbide for the tool, aluminium for the spindle and the forearm and steel for the rest of the robot structure. Lastly, a linear perturbation step was applied to complete a frequency analysis.

Figure 17 shows the first deformation mode which is a bending mode at f=44.265 [Hz] with a modal mass of 296.67 [kg].

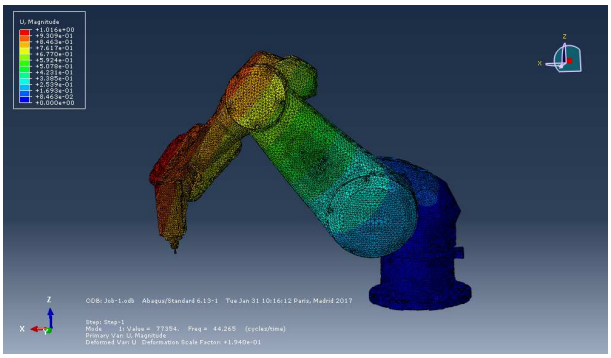

FIGURE 17: Finite element model of the machining robot

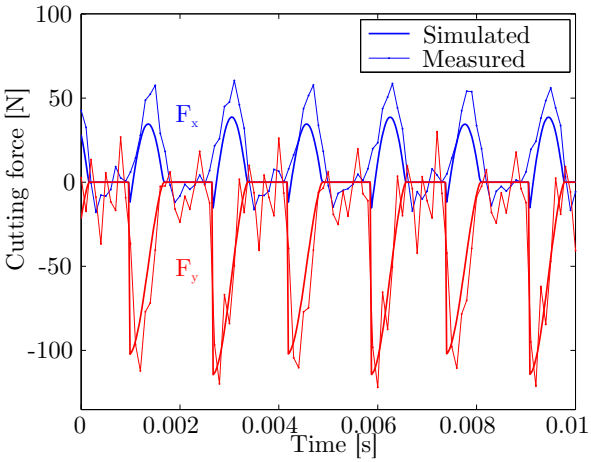

FIGURE 18: Fitting of the cutting forces at a_p=1.6 mm in down-milling

Although finding a stiffness of 23 [N/μm] is high due to the non-inclusion of the joint stiffness, these modal characteristics were still entered in the cutting force model since no other modal mass information was available.

Model fitting

Using fixed modal characteristics and cutting coefficients, the cutting force model was fitted to the unfiltered measurements for all axial depths of cut in down- and up-milling operations. Since the spatial discretisation of the machining model includes a representation of the tool, its tooth variable pitch was taken into account in the simulation. As can be seen in figure 18 for a down-milling operation at a_p=1.6 [mm], the model is able to match the measurements quite well. Especially for F_y, since each tooth removed a slight different amount of material due to the variable pitch, the steady state cutting forces oscillated between -100 [N] and -110 [N]. This trend was well represented by the model. The same conclusion could be drawn for the other fittings.

CONCLUSION AND FUTURE WORK

This short communication reported on an analysis of results obtained through surfacing robotic machining operations into an aluminium plate using a Stäubli TX200 robot. A first metrological analysis was carried out on the machined part and indicated that the smooth milled surface presented an arithmetic roughness between 0.4 and 0.8 [μm]. Its evaluated flatness around 0.238 [mm] also constituted a good result for robotic machining applications. After having analysed the vibration signals with a FFT, the measured cutting forces were examined to identify global cutting coefficients. It is worth to notice that all measurements provided cutting coefficient values in the same range which demonstrates that the considered robot is able to mill aluminium parts without any instability, at least up to an axial depth of cut of 1.6 [mm].

A cutting force model was then fitted to the measurements. In order to identify its dynamic parameters (mass, damping and stiffness), a finite element model was achieved on Abaqus software. The damping ratio was found by examining the decline in cutting forces at the end of each pass. The matching with the measurements using a simple mass-spring-damper system to represent the robot dynamic turned out to be acceptable in steady state.

Although the dynamic effects where not clearly visible since the model fitting was achieved in steady state, authors feel that it will be more convenient to actually identify the real dynamics properties of the robot through hammer shots during a future measurement campaign. It will allow verifying whether robot eigen frequencies are around 10 [Hz] as stated in the literature.

Authors are also aware that the finite element model should be improved by replacing the TIE constraints, freezing all DOF between the parts, by 'bushings' which will lead to a more realistic stiffness for the robot. A structural analysis of the robot, similar to the one found in [18] could also be achieved. Authors finally hope that this analysis of measurements will benefit to researchers trying to characterise robotic machining phenomena.

ACKNOWLEDGMENT

The authors would like to thanks the Belgian National Fund for Scientific Research (NFSR-FRIA) for the financial support and the CNCSolutions - VDS company, which is specialised in design, integration and commercialisation of machines such as machining robots, as well as special machines built according to client's requirements, for the access granting to their machining robot.

REFERENCES

[1] John Pandremenos, Christos Doukas, Panagiotis Stravopoulos, George Chryssolouris, 2011. "Machining with robots: a critical review". *7th International Conference on Digital Enterprise Technology,* **Proceedings of DET2011**.

[2] S. Caro, C. Dumas, S. Garnier, B. Furet, May, 2013. "Workpiece placement optimization for machining operations with a kuka kr270-2 robot". *IEEE International Conference on Robotics and Automation (ICRA)*, pp. 2921–2926.

[3] I. Iglesias, M.A. Sebastian, J.E. Ares, 2015. "Overview of the state of robotic machining: Current situation and future potential". *Procedia Engineering,* **132**, pp. 911–917.

[4] Z. Pan, H. Zhang, Z. Zhu, J. Wang, 2006. "Chatter analysis of robotic machining process". *Journal of Material Processing Technology*, **173**, pp. 301–309.

[5] H. Zhang, J. Wang, G. Zhang, Z. Gan, Z. Pan, H. Cui, Z. Zhu, USA, July, 2005. "Machining with flexible manipulator: Toward improving robotic machining performance". *Proc. IEEE-ASME International Conference on Advanced Intelligent Mechatronics*, pp. 1127–1132.

[6] U. Schneider, M. Drust, A. Puzik, A. Verl, 2013. "Compensation of errors in robot machining with a parallel 3d-piezo compensation mechanism". *Procedia CIRP,* **7**, pp. 305–310.

[7] Mohamed Slamani, Sébastien Gauthier, Jean-François Chatelain, 2016. "Comparison of surface roughness quality obtained by high speed CNC trimming and high speed robotic trimming for CFRP laminate". *Robotics and Computer-Integrated Manufacturing*, **42**, pp. 63–72.

[8] A. Abele, M. Weigold, S. Rothenbücher, 2007. "Model and identification of an industrial robot for machining applications". *Annals of CIRP,* **56-1**, pp. 387–390.

[9] S. G. Mousavi, V. Gagnol, B.C. Bouzgarou, P. Ray, July, 2013. "Dynamic behaviour model of a machining robot". *ECCOMAS Multibody Dynamics*, pp. 771–779.

[10] C. Dumas, S. Caro, S. Garnier, B. Furet, 2011. "Joint stiffness identification of six-revolute industrial serial robots". *Robotics and Computer-Integrated Manufacturing*, **27**, pp. 881–888.

[11] N.R. Slavkovic, D.S. Milutinovic, M.M. Glavonjic, 2014. "A method for off-line compensation of cutting force-induced errors in robotic machining by tool path modification". *Int J Adv Manuf Technol, Springer,* **70**, pp. 2083–2096.

[12] U. Schneider, M. Ansaloni, M. Drusti, 2013. "Experimental investigation of sources of error in robot machining". *CCIS,* **371**(1), pp. 14–26.

[13] Y. Altintas, 2000. "Manufacturing automation, metal cutting mechanics, machine tool vibrations, and cnc design". *Cambridge University press.*

[14] E. Rivière, E. Filippi, P. Dehombreux, 2007. "Inverse Method for cutting forces parameters evaluation". *Engineering MECHANICS*, **5**, pp. 1–13.

[15] S. Engin, Y. Altintas, 2001. "Mechanics and dynamics of general milling cutters. Part I: helical end mills". *International Journal of Machine Tools and Manufacture*, **41**, pp. 2195–2212.

[16] E. Rivière, E. Filippi, P. Dehombreux, (Fifth International Conference on High Speed Machining (HSM 2006)), Mars, Metz, France 2006. "Forces, vibrations and roughness prediction in milling using dynamic simulation". *Proceedings*.

[17] E. Rivière, E. Filippi, P. Dehombreux, 2007. "Chatter prediction using dynamic simulation". *International Review of Mechanical Engineering (I.RE.M.E.),* **1**, pp. 78–86.

[18] C. Doukas, J. Pandremenos, P. Stravopoulos, P. Foteinopoulos, G. Chryssolouris, 2012. "On an empirical investigation of the structural behaviour of robots". *45th CIRP Conference on Manufacturing System,* **Procedia CIRP**, pp. 501–506.